



Microstructure, physical and soldering properties of Tin-Zinc-Bismuth alloy

Abu Bakr El-Bediwi*, Amira El-Shafei, Mustafa Kamal

Metal Physics Lab., Physics Department, Faculty of Science, Mansoura University, (EGYPT)

E-mail : baker_elbediwi@yahoo.com

ABSTRACT

The aim of present work was to improve physical and soldering properties of tin- zinc alloy and produce new Sn-Zn-Bi alloy with superior soldering properties for electronic applications. To verify this aims microstructure, electrical resistivity, elastic modulus, internal friction, thermal diffusivity, melting point and wetting behavior of $\text{Sn}_{96-x}\text{Zn}_4\text{Bi}_x$ ($x=0, 6, 12, 18, 24$ and 30) alloys have been investigated. Melting point, elastic modulus and thermal diffusivity values of $\text{Sn}_{96}\text{Zn}_4$ alloy decreased but electrical resistivity and internal friction values increased after adding bismuth content. Wetting behavior, contact angle, of $\text{Sn}_{96}\text{Zn}_4$ alloy varied after adding bismuth content. The $\text{Sn}_{72}\text{Zn}_4\text{Bi}_{24}$ lead free solder alloy has the best soldering properties for electronic application compared to commercial Pb- Sn alloy.

© 2015 Trade Science Inc. - INDIA

KEYWORDS

Microstructure;
Melting point;
Contact angle;
Elastic modulus;
Internal friction;
Thermal diffusivity;
Sn- Zn- Bi alloy.

INTRODUCTION

There are many different types of solder being used by industry. Solders are available in various forms that include bars, wires, ingots, and powders. Soldering is technically defined as the joining of two base materials through the use of a third “filler” metal with a melting temperature well below those of the substrates and typically less than 450°C . Solder alloys are categorized as either soft or hard. Soft solders typically contain tin and lead, although indium, cadmium, and bismuth are also found in soft solders. Hard solders contain metals such as gold, zinc, aluminum, and silicon. A more rigorous classification is based on the melting temperature where soft solders melt below approximately 350°C while hard solders melt above 350°C . Due to the inherent toxicity

of lead, environmental regulations around the world have been targeted to eliminate the usage of Pb-bearing solders in electronic assemblies. This has prompted the development of “Pb-free” solders, and has enhanced the research activities in this field. Lead-free solders in commercial use may contain tin, copper, silver, bismuth, indium, zinc, antimony, and traces of other metals. Sn-Zn solder alloy containing about 9 wt. % zinc (eutectic composition) has been proposed as a lead-free solder material which is expected to be put into practical use for reflow soldering. Those Sn-Zn solder alloys have advantages such that a eutectic temperature of a tin-zinc alloy is equal to 199°C , closest to a eutectic point of a tin-lead alloy among Sn-based lead-free solder alloys and costs of raw materials of them are lower than those of the other lead-free solder alloys. The influence

Full Paper

of adding cadmium content on structure and physical properties of SnZn₉ alloy has been investigated by El-Bediwi et al^[1]. Also thermodynamic properties and phase equilibrium relationship of Sn-Bi-Zn lead free solder alloys are determined experimentally and theoretically by Yang et al^[2]. Adding Ag to Sn-9Zn alloy inhibits the anodic dissolution of Zn and enhances the wettability of the solder alloy on Cu substrate^[3]. The effect of RE elements on the microstructure, mechanical properties, wetting behavior of certain Pb-free solder alloys reported and summarized^[4]. Several research^[5-7] studied eutectic tin- silver lead free solder alloy. The results show that, the eutectic SnAg_{3.5} is regarded as a good lead free solder alloy for certain aspects such as superior fatigue properties. Also structure, electrical resistivity, wettability, melting point and elastic modulus of Sn₅₀In₅₀, Sn_{72.2}In₂₀Ag_{2.8}, Sn_{72.5}In₂₅Ag_{2.5} and Sn₉₅Ag₅ lead free solder alloys have been investigated^[8]. The results show that, adding silver decreased electrical resistivity and wetting and increase melting point and elastic modulus of tin-indium. Adding In from 0 to 3 wt. % to Sn-0.3Ag-0.7Cu lead-free solder alloy lowered its solidus and liquidus temperatures with increasing melting range. Also wetting time of alloy is reduced with increased wetting force by increasing In content^[9]. Indium is a useful element to solve the problem of high melting point and low wettability of solder on Cu substrate^[10,11]. Microstructure, thermal properties, corrosion and oxidation resistance of Sn-9Zn-0.5Ag-1In solder alloy were studied^[12]. Adding 1% of In to Sn-9Zn-0.5Ag alloy decreased melting point of alloy and enhanced adhesion strength of alloy on Cu substrate. Also Sn-In-Ag system offers several advantages such as good wettability^[13,14], good corrosion behavior^[15] and very satisfying interaction with the substrate, especially with copper^[16].

Many studies have been made on various solders alloy based on Sn, e.g., Sn-9Zn, Sn-3.5Ag, Sn-3Ag-0.5Cu, etc. as likely substitutes^[17-19]. The properties of two lead free solder alloys, Sn-3.5% Ag-1% Zn and Zn-In, are described by M. Mc Cormack et al^[20]. Solidification behaviors of Sn-9Zn-XAg lead-free solder alloys are examined^[21]. Structure, electrical resistivity, wettability, melting point and elastic modulus of 50Sn-50In, 72.2Sn-20In-2.8Ag, 72.5Sn-25In-2.5Ag and

95Sn-5Ag lead free solder alloys have been investigated^[22]. A big problem with lead-free solder is that the higher the tin content, the more likely the growth of “tin whiskers”. Solders with 60% tin or more are called fine solders and are used in instrument soldering where temperatures are critical. The aim of this work is to improve physical and soldering properties of Sn₉₆Zn₄ alloy. Also to produce new Sn-Zn-Bi alloy with superior soldering properties by adding bismuth to tin-zinc alloy.

EXPERIMENTAL WORK

In the present work, Sn_{96-x}Zn₄Bi_x (x=0, 6, 12, 18, 24 and 30 wt.%) were melted in a muffle furnace using tin, zinc and bismuth of purity better than 99.5 %. The resulting ingots were turned and re-melted four times to increase the homogeneity. From these ingots, long ribbons of about 4 mm width and ~70 μm thickness were prepared by a single roller method in air (melt spinning technique). The surface velocity of the roller was 31.4 m/s giving a cooling rate of ~3.7 × 10⁵ K/s. The samples then cut into convenient shape for the measurements using double knife cutter. Microstructure of used samples was performed on the flat surface of all samples using an Shimadzu X-ray Diffractometer (Dx-30, Japan) of Cu-Kα radiation with λ=1.54056 Å at 45 kV and 35 mA and Ni-filter in the angular range 2θ ranging from 0 to 100° in continuous mode with a scan speed 5 deg/min. The electrical resistivity was measured by a conventional double bridge method. The differential thermal analysis (DTA) thermographs were obtained by SDT Q600 V20.9 Build 20 instrument with heating rate 10 °k/min. The internal friction Q⁻¹ and the elastic constants were determined using the dynamic resonance method. The value of the dynamic Young modulus *E* is determined by the following relationship^[22-24]:

$$\left(\frac{E}{\rho}\right)^{1/2} = \frac{2\pi L^2 f_0}{kz^2}$$

Where ρ the density of the sample under test, L the length of the vibrated part of the sample, k the radius of gyration of cross section perpendicular to its plane of motion, f₀ the resonance frequency and z the constant depends on the mode of vibration and is

equal to 1.8751. From the resonance frequency f_0 at which the peak damping occurs, the thermal diffusivity, D_{th} , can be obtained directly from the following equation:

$$D_{th} = \frac{2d^2f_0}{\pi}$$

Where d is the thickness of the sample

Plotting the amplitude of vibration against the frequency of vibration around the resonance f_0 gives the resonance curve, the internal friction, Q^{-1} , of the sample can be determined from the following relationship:

$$Q^{-1} = 0.5773 \frac{\Delta f}{f_0}$$

Where Δf the half width of the resonance curve

RESULTS AND DISCUSSION

X-ray analysis

X-ray diffraction patterns of $Sn_{96-x}Zn_4Bi_x$ ($x=0,$

6, 12, 18, 24 and 30) melt spun alloys have lines corresponding to sharp lines of body-centered tetragonal Sn phase, rhombohedral Bi phase and rhombohedral SnBi intermetallic phase. X-ray diffraction patterns and its analysis, Figure 1, for $Sn_{96}Zn_4$ show that, it consisted of β -Sn phase. But x-ray diffraction patterns and its analysis, Figure 1, of $Sn_{96-x}Zn_4Bi_x$ ($x=6, 12, 18, 24$ and 30) melt spun alloys show that, they consisted of β -Sn phase, rhombohedral Bi phase and rhombohedral SnBi intermetallic compound and that agreed with pervious results^[25,26].

From x-ray analysis it clear that, $Sn_{96}Zn_4$ alloy consisted of β -Sn phase. That is mean Zn atoms dissolved in Sn matrix forming β -Sn phase with a solid solution appeared as β -Sn phase with fine Zn-rich phases are dispersed in the Sn matrix near to the interface. Bi phase and SnBi intermetallic compound with β -Sn phase formed after adding bismuth content to $Sn_{96}Zn_4$ alloy. Also matrix microstructure of $Sn_{96}Zn_4$ alloy, such as crystallinity (which is related

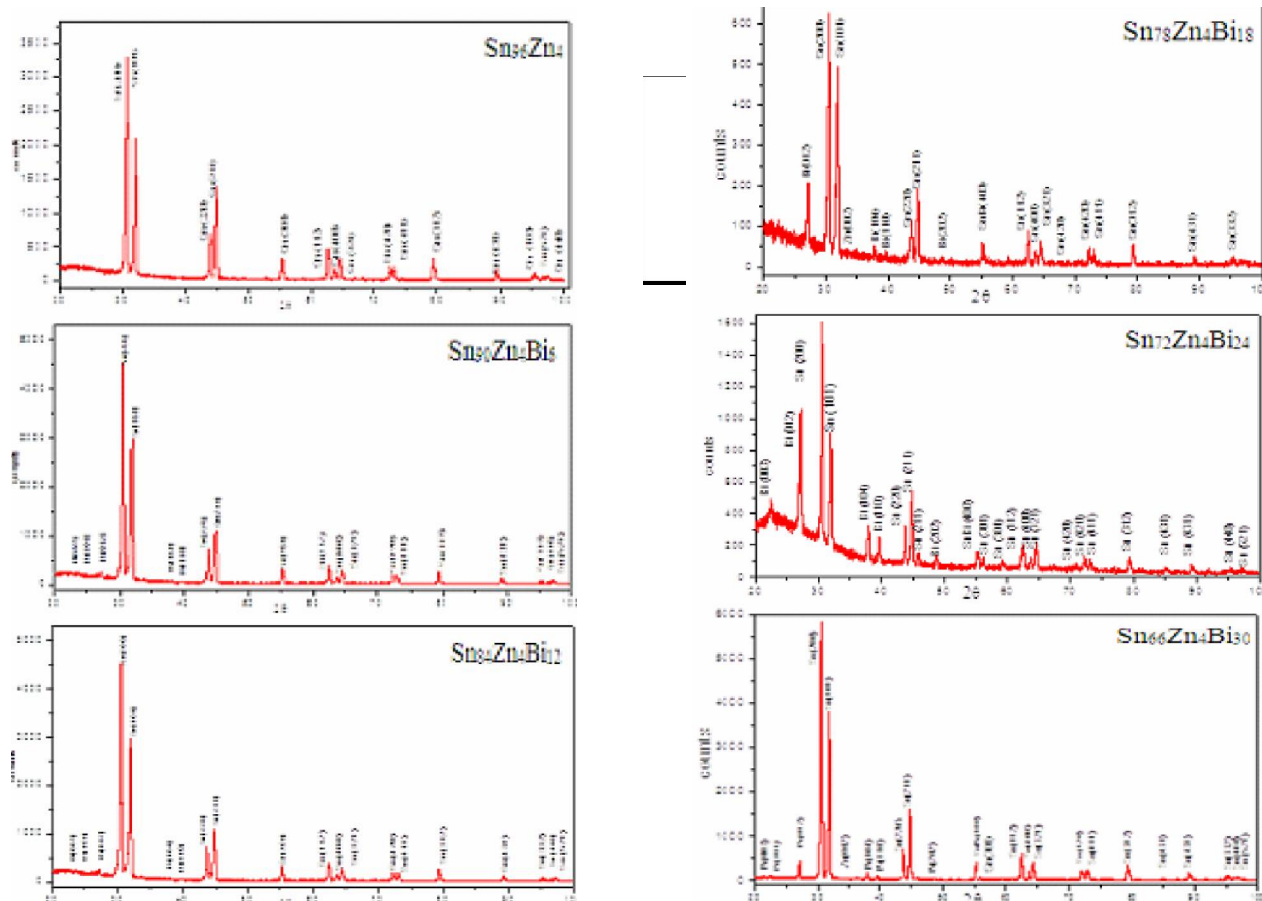


Figure 1 : x-ray diffraction patterns of $Sn_{96-x}Zn_4Bi_x$ alloys

Full Paper

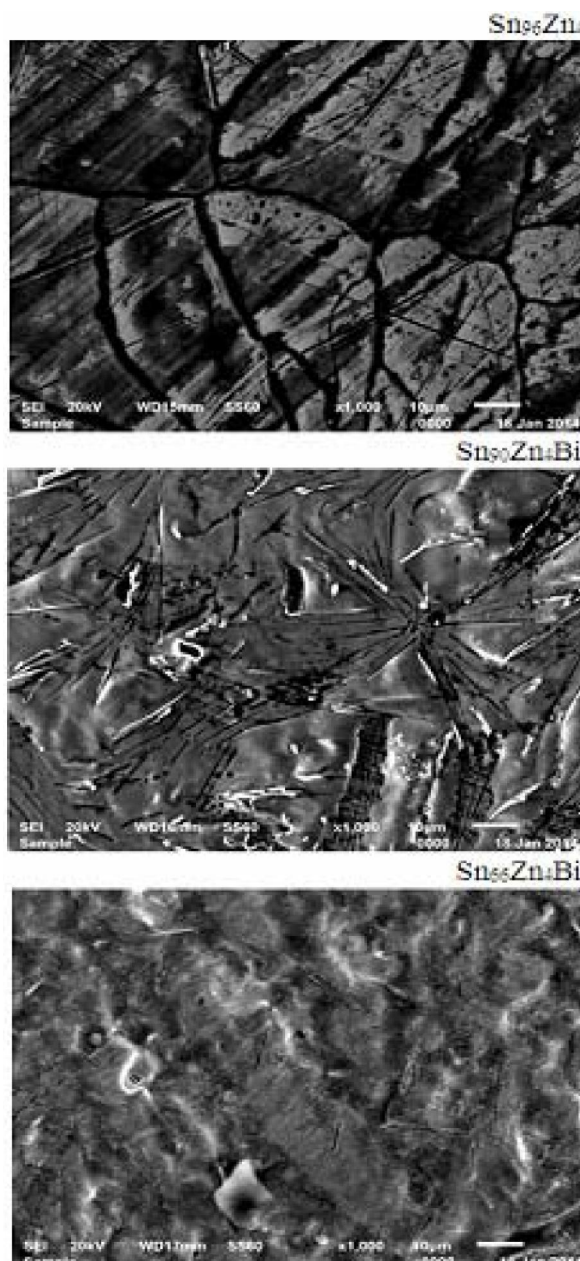


Figure 2 : Scanning electron micrographs of $\text{Sn}_{96-x}\text{Zn}_4\text{Bi}_x$ alloys

to intensity of the peak), crystal size (which is related to full width half maximum), the orientation (which is related to the position of the peak, 2θ), change after adding bismuth content.

Scanning electron microscope

Scanning electron micrographs, SEM, of $\text{Sn}_{96-x}\text{Zn}_4\text{Bi}_x$ ($x=0, 6$ and 30) alloys are shown in Figure 2. SEM analysis of $\text{Sn}_{96-x}\text{Zn}_4\text{Bi}_x$ ($x=0, 6$ and 30) alloys showed considerable heterogeneity of micro-structure, which will relate to the formation of non-equilibrium

phases. Three types of phases, (β -Sn phase) or (β -Sn phase, Bi phase and SnBi intermetallic compound), of various chemical compositions were discovered, which was also proved by the x-ray analysis.

Soldering properties

Wettability

Wettability is quantitatively assessed by the contact angle formed at the solder substrate's flux triple point. The contact angles of $\text{Sn}_{96-x}\text{Zn}_4\text{Bi}_x$ ($x=0, 6, 12, 18, 24$ and 30) alloys on pure Cu substrate are shown in TABLE 1. From these results, it is clear that a significant change in contact angle, wettability, of $\text{Sn}_{96}\text{Zn}_4$ alloy after adding bismuth content and that is agree with previous results^[27,28]. The $\text{Sn}_{72}\text{Zn}_4\text{Bi}_{24}$ alloy has lower contact angle, good wetting on pure Cu substrate. The spreading of $\text{Sn}_{96-x}\text{Zn}_4\text{Bi}_x$ ($x=0, 6, 12, 18, 24$ and 30) alloys on pure Cu at room temperature in air is shown in Figure 3.

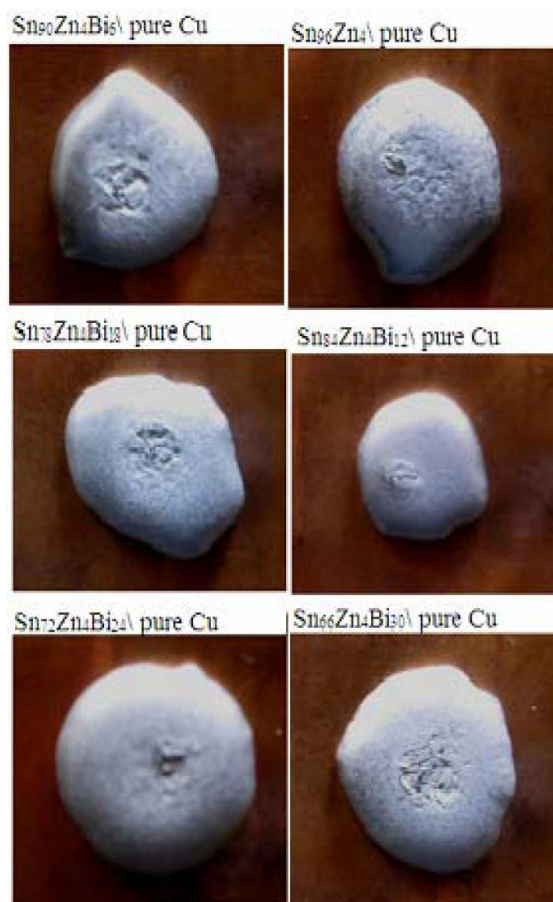
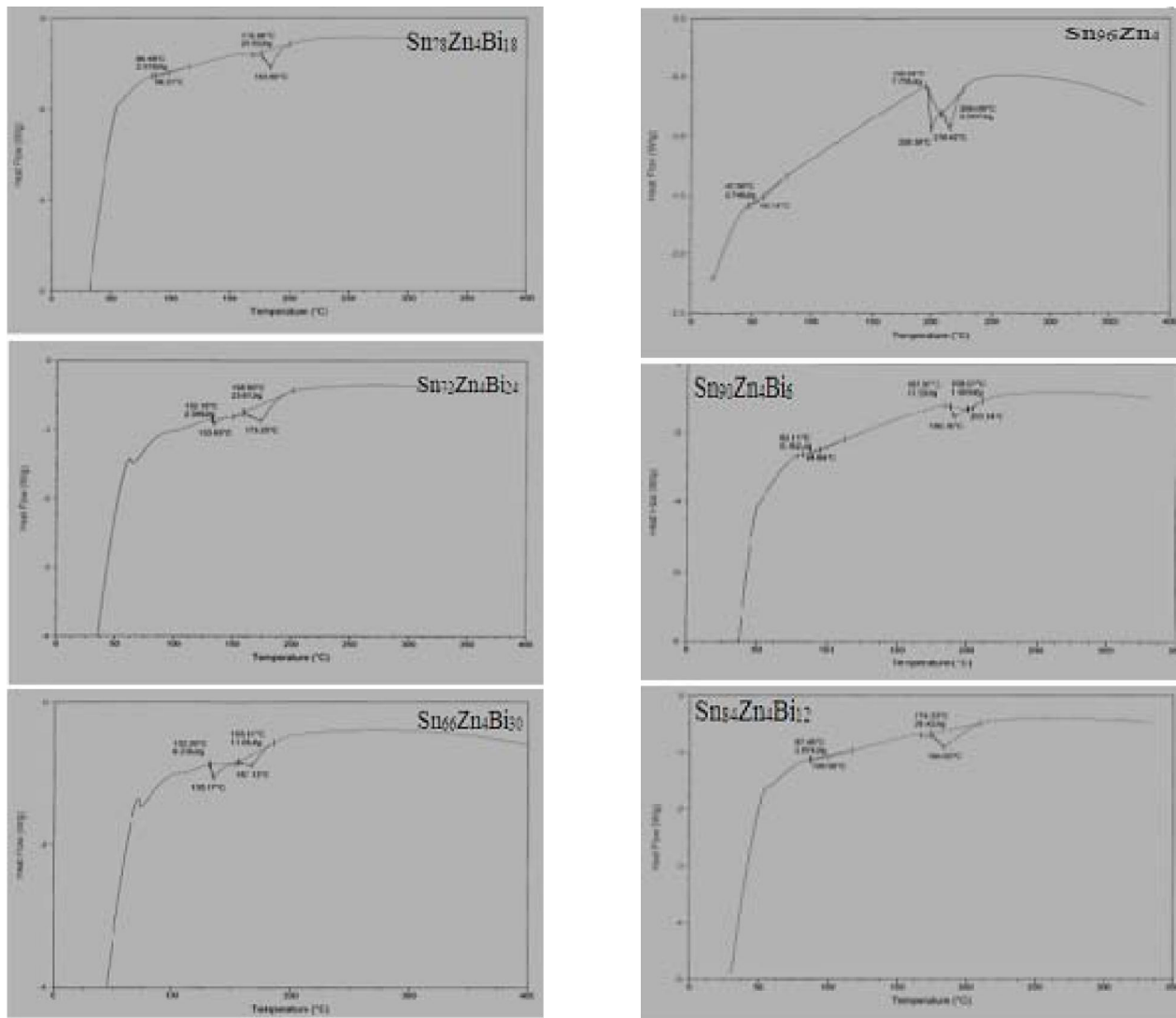


Figure 3 : spreading of $\text{Sn}_{96-x}\text{Zn}_4\text{Bi}_x$ alloys on pure Cu at room temperature in air

Figure 4 : DSC thermographs of $\text{Sn}_{96-x}\text{Zn}_4\text{Bi}_x$ alloysTABLE 1: Contact angles of $\text{Sn}_{96-x}\text{Zn}_4\text{Bi}_x$ alloys

Alloys	Contact angle θ°
$\text{Sn}_{96}\text{Zn}_4$	61.5 ± 3
$\text{Sn}_{90}\text{Zn}_4\text{Bi}_6$	80 ± 8
$\text{Sn}_{84}\text{Zn}_4\text{Bi}_{12}$	59 ± 2
$\text{Sn}_{78}\text{Zn}_4\text{Bi}_{18}$	75 ± 5
$\text{Sn}_{72}\text{Zn}_4\text{Bi}_{24}$	57 ± 1.5
$\text{Sn}_{66}\text{Zn}_4\text{Bi}_{30}$	78 ± 5

Melting point

Thermal analysis is often used to study solid state transformations as well as solid-liquid reactions. The melting temperature is an important physical property and has a great influence on printed circuit board assembly. A promising solder alloy should have a lower melting temperature and a narrow pasty temperature

zone. Figure 4 shows the DSC thermographs of $\text{Sn}_{96-x}\text{Zn}_4\text{Bi}_x$ ($x=0, 6, 12, 18, 24$ and 30) alloys. From these graphs the melting point of Sn-Zn-Bi alloys are determined. The melting point of $\text{Sn}_{96-x}\text{Zn}_4\text{Bi}_x$ ($x=0, 6, 12, 18, 24$ and 30) alloys is listed in TABLE 2. Thermo-graphs of Sn-Zn-Bi alloys have a variation in their shape, exothermal peaks. That means

TABLE 2 : Melting temperature of $\text{Sn}_{96-x}\text{Zn}_4\text{Bi}_x$ alloys

Alloys	Melting temperature C°
$\text{Sn}_{96}\text{Zn}_4$	216.42
$\text{Sn}_{90}\text{Zn}_4\text{Bi}_6$	190.75
$\text{Sn}_{84}\text{Zn}_4\text{Bi}_{12}$	184
$\text{Sn}_{78}\text{Zn}_4\text{Bi}_{18}$	183.6
$\text{Sn}_{72}\text{Zn}_4\text{Bi}_{24}$	173.25
$\text{Sn}_{66}\text{Zn}_4\text{Bi}_{30}$	167.13

Full Paper

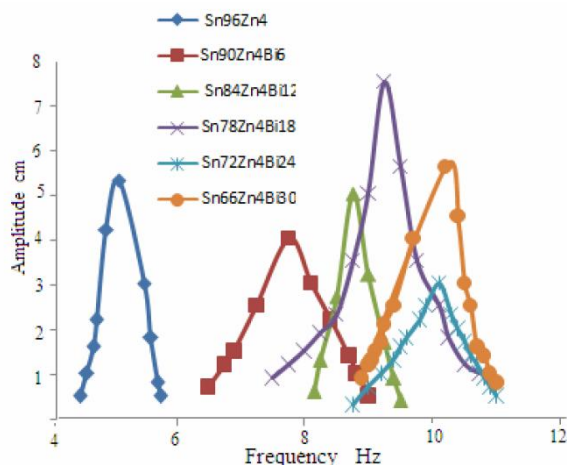


Figure 5 : Resonance curves of $\text{Sn}_{96-x}\text{Zn}_4\text{Bi}_x$ alloys

that, there is a change in alloys matrix structure caused after adding Bi content to $\text{Sn}_{96}\text{Zn}_4$ which agrees with the results seen in x-ray analysis and scanning electron micrographs. The melting temperature of $\text{Sn}_{96}\text{Zn}_4$ alloy decreased after adding bismuth content and that is agree with pervious results^[29]. The $\text{Sn}_{66}\text{Zn}_4\text{Bi}_{30}$ alloy has lowest melting point, 167.13°C, and it is lower than that the melting point of eutectic Sn-Pb solder alloy.

Electrical resistivity

In general, the plastic deformation raises the electrical resistivity as a result of the increased number of electron scattering centers. Crystalline defects serve as scattering center for conduction electrons in metals, so the increase in their number raises the imperfection. The measured electrical resistivity values of $\text{Sn}_{96-x}\text{Zn}_4\text{Bi}_x$ ($x=0, 6, 12, 18, 24$ and 30) alloys are listed in TABLE 3. Electrical resistivity value of $\text{Sn}_{96}\text{Zn}_4$ alloy increased after adding bismuth content as seen in TABLE 3. That is because Sn-Zn matrix microstructure, such as forming Bi phase, SnBi intermetallic compound with β -Sn phase, changed after adding bismuth content playing as scattering center for conduction electrons which in-

TABLE 3: Electrical resistivity of $\text{Sn}_{96-x}\text{Zn}_4\text{Bi}_x$ alloys

Alloys	$\rho \times 10^{-8} \text{ } \Omega \cdot \text{m}$
$\text{Sn}_{96}\text{Zn}_4$	36.08±1.9
$\text{Sn}_{90}\text{Zn}_4\text{Bi}_6$	46.08±2.01
$\text{Sn}_{84}\text{Zn}_4\text{Bi}_{12}$	57.41±3.15
$\text{Sn}_{78}\text{Zn}_4\text{Bi}_{18}$	64.08±3.75
$\text{Sn}_{72}\text{Zn}_4\text{Bi}_{24}$	68.83±4.1
$\text{Sn}_{66}\text{Zn}_4\text{Bi}_{30}$	82.73±4.23

creases their resistivity. Also bismuth is a semimetal with high resistivity.

Elastic properties

The elastic constants of solid are important for both fundamental and practical reasons. The elastic constants are directly related to atomic bonding and structure. It is also related to the atomic density. Elastic moduli of $\text{Sn}_{96}\text{Zn}_4$ alloy decreased after adding bismuth content as shown in TABLE 4. That is because the dissolved bismuth atoms on grain bound-

TABLE 4 : Elastic moduli of $\text{Sn}_{96-x}\text{Zn}_4\text{Bi}_x$ alloys

Alloys	E GPa	B GPa	μ GPa
$\text{Sn}_{96}\text{Zn}_4$	44.34±3.1	51.18	16.35
$\text{Sn}_{90}\text{Zn}_4\text{Bi}_6$	40.07±2.25	45.68	14.80
$\text{Sn}_{84}\text{Zn}_4\text{Bi}_{12}$	36.13±1.65	40.69	13.36
$\text{Sn}_{78}\text{Zn}_4\text{Bi}_{18}$	30.6±1.43	33.86	11.34
$\text{Sn}_{72}\text{Zn}_4\text{Bi}_{24}$	27.43±1.15	30.15	10.17
$\text{Sn}_{66}\text{Zn}_4\text{Bi}_{30}$	23.9±1.2	25.97	8.87

ary/ or the formed phases, Bi and SnBi, in Sn-Zn matrix affected on matrix bonding strengthen which decreased elastic modulus value of Sn-Zn alloy.

The resonance curves $\text{Sn}_{96-x}\text{Zn}_4\text{Bi}_x$ ($x=0, 6, 12,$

TABLE 5 : Internal friction and thermal diffusivity of $\text{Sn}_{96-x}\text{Zn}_4\text{Bi}_x$ alloys

Alloys	$D_{th} \times 10^{-4} \text{ cm}^2/\text{sec}^2$	Q^{-1}
$\text{Sn}_{96}\text{Zn}_4$	5.3	0.027±0.001
$\text{Sn}_{90}\text{Zn}_4\text{Bi}_6$	2.93	0.039±0.002
$\text{Sn}_{84}\text{Zn}_4\text{Bi}_{12}$	2.56	0.042±0.002
$\text{Sn}_{78}\text{Zn}_4\text{Bi}_{18}$	2.21	0.052±0.002
$\text{Sn}_{72}\text{Zn}_4\text{Bi}_{24}$	1.85	0.041±0.002
$\text{Sn}_{66}\text{Zn}_4\text{Bi}_{30}$	3.03	0.050±0.002

18, 24 and 30) alloys are shown in Figure 5. Calculated Internal friction and thermal diffusivity values are seen in TABLE 5. The results show that, internal friction value of Sn-Zn alloy increased but thermal diffusivity decreased after adding bismuth content.

CONCLUSION

- 1) X-ray diffraction patterns and its analysis for $\text{Sn}_{96}\text{Zn}_4$ alloy show that, it consisted of β -Sn phase. Bi phase, SnBi intermetallic compound and β -Sn phase are detected after adding Bi to $\text{Sn}_{96}\text{Zn}_4$

alloy. These crystal structure of formed phases, (shape, size and position) dependent on the alloy composition.

- 2) Melting temperature, elastic modulus and thermal diffusivity of $\text{Sn}_{96}\text{Zn}_4$ alloy decreased but electrical resistivity and internal friction increased after adding bismuth content.
- 3) Contact angle $\text{Sn}_{96}\text{Zn}_4$ alloy varied after adding bismuth content.
- 4) The $\text{Sn}_{72}\text{Zn}_4\text{Bi}_{24}$ alloy has best solder properties as lead free solder compared to Sn- Pb alloy.

REFERENCES

- [1] A.El-bediwi, M.M.El-Bahay, M.Kamal; radiation Effects & Defects in solids, **159**, 491-496 (2004).
- [2] C.Yang, F.Chen, W.Gierlotka, S.Chen, K.Hsieh, L.Huang; Materials Chemistry and Physics, **112**, 94-100 (2008).
- [3] T.Takemoto, T.Funaki, A.Matsunawa; J.Jap.Weld.Soc., **17**, 251-258 (1999).
- [4] C.M.L.Wu, D.Q.Yu, C.M.T.Law, L.Wang; Properties of lead-free solder alloys with rare earth element additions, Mater.Sci.and Eng.: R: Reports, **44(1)**, 1-44 (2004).
- [5] Y.Kariya, M.Otsuka; J.Electron.Mater, **27**, 866-70 (1998).
- [6] W.J.Tomlinson, A.Fullylove; J.Mater.Sci., **27**, 5777-81 (1992).
- [7] F.Ochoa, J.J.Williams, N.Chawla; J.Electron Mater, **32**, 1414-20 (2003).
- [8] A.El-Bediwi, M.M.El-Bahay; Radiation Effects & Defects in Solids, **159**, 133-40 (2004).
- [9] K.Kanlayasiri, M.Mongkolwongrojn; T.Ariga, J.of alloys and compounds, **485**, 225-230 (2009).
- [10] M.S.yeh; J.Electron.Mater, **30**, 953-956 (2002).
- [11] S.P.Yu, C.L.Liao, M.C.Wang, M.H.Hon; J.Mater.Sci., **35**, 1-8 (2001).
- [12] T.C.Chang, J.W.Wang, M.C.Wang, M.H.Hon; J.alloys & Comp., (2006).
- [13] D.R.Frear; J.Metals, **48(5)**, 49-53 (1996).
- [14] I.Artaki, A.M.Jackson, P.T.Vianco; J.Electron.Mater., **23(8)**, 757-64 (1994).
- [15] H.Oulfajrite, A.Sabbar, M.boulghallat, A.Touaiti, R.Lbibb, A.zrineh; Mater.Letters, **57**, 4368-71 (2003).
- [16] W.K.Choi, H.M.Lee; J.Korean., Phys.Soc., **35**, 340-344 (1999).
- [17] R.K.Shiue, L.W.Tsay, C.L.Lin, J.L.Ou; J.Mater.Sci., **38**, 1269 (2003).
- [18] A.Miiyamoto, T.Ogawa, T.Ohsawa; Mater.Sci.Res.Inter., **9**, 16 (2003).
- [19] A.B.El-Bediwi, M.El-Sayed, M.Kamal; Radiation Effects & Defects in Solids, **160(7)**, 297-300 (2005).
- [20] M.Mc Cormack, S.Jin, G.W.Kammlott, H.S.Chen; Appl.Phys.Lett., **63**, 15 (1993).
- [21] Y.L.Tsai, W.S.Hwang; Material Science and Engineering A, **413-414**, 312-316 (2005).
- [22] E.Schreiber, O.L.Anderson, N.Soga; Elastic constant and their measurements, McGraw-Hill, New York, **82**, (1973).
- [23] S.Timoshenko, J.N.Goddier; Theory of elasticity, 2nd Edition, McGraw-Hill, New York, **277**, (1951).
- [24] K.Nuttall; J.Inst.Met., **99**, 266 (1971).
- [25] J.Zhou, Y.Sun, F.Xue; J.Alloys Compd., **397**, 260-264 (2005).
- [26] S.W.Chen, C.H.Wang, S.K.Lin, C.N.Chiu; J.Mater.Sci.: Mater.Electron., **18**, 19-37 (2007).
- [27] A.Mulugeta, S.Guna; Mater.Sci.Eng., **27**, 95-141 (2000).
- [28] L.C.Prasad, A.Mikula; J.Alloys Compd., **282**, 279 (1999).
- [29] D.Soaes, C.Vilarinho, J.Barbosa, R.Silva, F.Castro; Effect of the Bi content on the interface reactions between copper substrate and Sn-Zn-Al-Bi lead-free solder, IX Conference on Metallurgical Science and Technology, Madrid, 5-7 November, (2003).